Phonon-assisted tunneling from a two-dimensional emitter state

P. J. Turley and S. W. Teitsworth
Department of Physics, Box 90305, Duke University, Durham, North Carolina 27708-0305
(Received 17 December 1993; revised manuscript received 13 June 1994)

We present a theory of phonon-assisted tunneling in GaAs/AlAs double-barrier structures, which treats the electrons in the emitter as a two-dimensional electron gas. A complete set of confined and interface optical-phonon modes is calculated using a dielectric-continuum model, and we derive a general expression for the electron-phonon Hamiltonian valid for all optical-phonon modes in an arbitrary heterostructure. The electronic wave functions relevant to phonon-assisted tunneling are found by self-consistently solving the Schrödinger and Poisson equations in both the well and the emitter. Five different phonon modes are predicted to dominate the phonon-assisted tunneling current: three LO-like interface modes, the half-space modes in the emitter, and the confined modes in the well.

I. INTRODUCTION

Phonon-assisted tunneling (PAT) in double-barrier structures has attracted a great deal of experimental[1–9] and theoretical[8–22] interest over the past few years. From a device standpoint low levels of PAT are desirable in order to increase peak-to-valley current ratios, while from a fundamental view phonon-assisted tunneling measurements provide a means for testing models of localized optical phonons and associated electron-phonon interactions in quantum-well structures.

While there are numerous theoretical studies of PAT in double-barrier structures,[8–22] few of these make detailed comparisons to experiment. Some do not include localized phonons in the calculations, while others simplify too drastically the dynamics of electrons in the emitter region of the device. Usually, the electrons in the emitter region of a double-barrier device are modeled as a three-dimensional electron gas in equilibrium. However, this is inappropriate for many devices, which often contain undoped spacer layers outside the two barrier layers. The introduction of spacer layers has been shown to improve the peak-to-valley ratio of devices through the formation of a two-dimensional electron gas in the emitter.[23] To accurately model the PAT curve at low temperatures in realistic double-barrier structures, it is therefore essential to treat both the two-dimensional electron gas in the emitter and the localized phonons.

Recently, Turley *et al.*[9] compared experimental current-voltage curves from a GaAs/AlAs double-barrier structure to model calculations which included both localized phonons and a two-dimensional emitter state. In that paper, close agreement between theory and experiment was demonstrated, confirming the existence of interface modes in a double-barrier structure. The phonon properties were treated using the dielectric-continuum model, a simple macroscopic model of localized optical phonons in which the phonon properties are described in terms of the bulk dielectric properties of the various semiconductor layers.[24]

In this paper we describe in detail the model used in Ref. 9 for calculating the PAT current from a two-dimensional emitter state with all localized optical-phonon modes included. In Sec. II we describe the calculation of the electronic wave functions and discuss the basic PAT current formula for a two-dimensional electron gas in the emitter. In Sec. III we use the dielectric-continuum model to derive a general expression for the electron-phonon Hamiltonian valid for all localized optical-phonon modes in an arbitrary heterostructure. In Sec. IV we calculate the PAT current using a method which is more computationally efficient than those described in previous papers.[14,16] The results of these calculations are presented and discussed in Sec. V.

The experimental double-barrier device that we are modeling consists of an 80-Å GaAs well, surrounded by a 33-Å AlAs barrier on one side and a 45-Å AlAs barrier on the other. Asymmetric structures have been shown to give large PAT peaks relative to the resonant tunneling peak.[2,9,20] Detailed descriptions of the spacer layers and growth procedures are given in Ref. 9. We assume that the temperature is low enough (typically $T=4$ K for the relevant experimental results) to make the approximation $T=0$.

II. ELECTRONIC STATES

In the phonon-assisted tunneling process, electrons are transferred from the emitter of the double-barrier structure to the well by the emission of an optical phonon. The phonon emission rate can be calculated using the Fermi golden rule:

$$W(i\rightarrow f)=\frac{2\pi}{\hbar}|\langle f|H_{e\text{-ph}}|i\rangle|^2\delta(E_i-E_f-\hbar\omega)\ , \qquad (2.1)$$

where the Hamiltonian $H_{e\text{-ph}}$ describes the interaction between the electrons and the optical phonons, E_i is the energy of the initial electronic state, E_f is the energy of the final electronic state, and $\hbar\omega$ is the energy of the phonon. The *total* initial state $|i\rangle$ has one electron in state Ψ_i with no phonons, while the *total* final state $|f\rangle$ consists of one electron in the state Ψ_f plus one emitted phonon.

In the absence of a magnetic field the initial and final electronic states are written

$$\Psi_i(r)=\frac{e^{i\mathbf{k}_\parallel\cdot\mathbf{r}_\parallel}}{\sqrt{A}}\varphi_i(z) \tag{2.2}$$

and

$$\Psi_f(r)=\frac{e^{i\mathbf{k}'_\parallel\cdot\mathbf{r}_\parallel}}{\sqrt{A}}\varphi_f(z)\ ,$$

where A is the cross-sectional area of the entire structure, $\varphi_i(z)$ and $\varphi_f(z)$ are the z-dependent parts of the wave function, and $\mathbf{r}_\parallel$ and $\mathbf{k}_\parallel$ are, respectively, the position and wave vector projected onto the plane of the interfaces, i.e., $\mathbf{k}=\mathbf{k}_\parallel+k_z\hat{\mathbf{z}}$. ($\mathbf{k}$ is the total momentum of the electron and $\hat{\mathbf{z}}$ is the unit vector in the z direction.)

The emission rate is summed over all available initial and final states to calculate the current. For a two-dimensional electron gas in the emitter, the current is given by

$$J(V)=\frac{e}{A}\int d\mathbf{k}'_\parallel\int d\mathbf{k}_\parallel W(i\rightarrow f;V)g_w(\mathbf{k}'_\parallel)g_e(\mathbf{k}_\parallel) \times f_e(\mathbf{k}_\parallel)[1-f_w(\mathbf{k}'_\parallel)]\ , \tag{2.3}$$

where $g_e(\mathbf{k}_\parallel)=2(A/(2\pi)^2)$ is the density of electronic states in the emitter, $g_w(\mathbf{k}'_\parallel)=(A/(2\pi)^2)$ is the density of available electronic states in the well (the factor of 2 is dropped because the electrons do not change spin during phonon emission), A is the cross-sectional area of the device, $f_e(\mathbf{k}_\parallel)$ is the distribution of electrons in the emitter, and $f_w(\mathbf{k}'_\parallel)$ is the distribution of electrons in the quantum well. The $[1-f_w(\mathbf{k}'_\parallel)]$ factor in this equation accounts for the reduction of current due to the Pauli exclusion principle.[20,22]

We determine the z-dependent parts of the wave function by simultaneously solving the Schrödinger and Poisson equations in the well and emitter. We only look at contributions from two states, the lowest energy quasi-bound state in the well, and the lowest energy quasi-bound state in the emitter, both of which are effectively two-dimensional. At low temperatures the higher energy states in the emitter are essentially unoccupied, and in GaAs/AlAs double barrier structures current from the higher energy emitter states is only detected at higher temperatures.[25,26]

The total charge in the well is given by the formula $n_w=J\tau_w$, where n_w is the charge density in the well, J is the current, and τ_w is the lifetime of carriers in the well. The lifetime of carriers in the well is determined by the rate of tunneling through the collector barrier, and is calculated using a simple one barrier tunneling formula.[27] Once the charge in the well is known, the charge in the emitter is calculated using

$$\varepsilon_0\kappa_0\mathcal{E}_c=n_w+n_e\ , \tag{2.4}$$

where n_e is the charge density in the emitter, $\mathcal{E}_c$ is the magnitude of the electric field in the collector barrier, κ_0 is the static dielectric constant in the barrier, and ε_0 is the permittivity of free space.

Because the electron-electron scattering time (≈ 100 fs) is much shorter than the lifetime of electrons in the well or emitter (≈ 5 ns in this structure), the distribution of electrons is given by a Fermi distribution with a well-defined electron temperature. Because the acoustic-phonon emission time (<0.1 ns) is also much shorter than the electron lifetime, it is reasonable to assume that the electron temperature is the same as the lattice temperature,[9] though this assumption may not be valid in structures with thinner barriers.

We self-consistently solve the Schrödinger and Poisson equations to determine the z energy of the initial state E_z, the z energy of the final state E_{zf}, and the z-dependent parts of the wave functions. The current may then be calculated using Eq. (2.3). The total voltage drop is determined by adding the voltage drop across the collector (calculated using the depletion layer approximation) to the voltage drop across the barriers, well, and emitter (calculated using the Schrödinger and Poisson equations). The results from the first current calculation are used to recalculate n_w and n_e, and the procedure is repeated until convergence is satisfactory, which generally requires no more than 12 iterations.

Figure 1 shows two plots of the wave functions and potential profile calculated using a simultaneous solution of the Schrödinger and Poisson equations. Figure 1(a) shows the wave functions plotted on a linear scale (grey lines) and the potential profile (solid line). Figure 1(b) shows the wave functions plotted on a logarithmic scale with an expanded view of the potential profile. The two horizontal solid lines denote the z energy of the initial and final states. The z-energy separation between the two states ΔE_z has also been noted in the figure. It is impor-

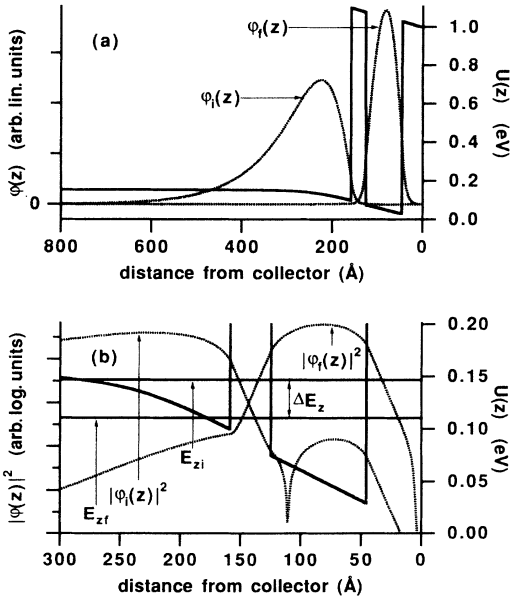

FIG. 1. Calculated initial wave function, final wave function, and conduction-band-edge profile using a simultaneous Schrödinger-Poisson solution: (a) The wave functions plotted on a linear scale (gray lines) and the potential profile (solid line). (b) The wave functions plotted on a logarithmic scale and an expanded view of the potential profile. The two horizontal solid lines denote the energies of the initial and final states with respect to the potential profile.

tant to realize that the initial and final wave functions overlap in the emitter in addition to the barriers and well. Most previous calculations ignored the overlap of the wave functions in the emitter, including those presented in Ref. 9, but we find that the overlap in the emitter can be crucial in determining which phonon modes contribute to the PAT current.[28]

III. ELECTRON-PHONON HAMILTONIANS

The electron-phonon interaction in semiconductor microstructures has been described using a number of theoretical techniques. Several microscopic approaches have been developed which look directly at the forces among the lattice atoms,[29–32] but the results of these calculations are often too complicated to incorporate easily into an electronic transport calculation. For transport purposes it is advantageous to use a macroscopic continuum picture. Accordingly, we adopt the dielectric-continuum model, which calculates the polar-optical phonon modes in terms of the corresponding bulk dielectric properties of the different material layers. Recent microscopic calculations have shown that this model provides an accurate description of the phonon modes in quantum wells, especially for longer wavelength phonons which are most important for electron scattering.[31]

Although numerous derivations of the electron-phonon Hamiltonians within the dielectric continuum model exist,[33–37] most of these are rather complicated and specific to a particular type of heterostructure. For this reason, we include a straightforward derivation of a general expression for the electron-localized phonon Hamiltonian which is applicable to arbitrary heterostructures.

In polar semiconductors, optical phonons polarize the semiconductor, generating an electromagnetic field. Since induction effects are quite small for the phonon wavelengths of interest, the electric field due to the phonon is well described by a scalar potential $\Phi(\mathbf{r})$.[16] The interaction energy of an electron with charge e in the phonon field is then written $H_{e\text{-ph}}=e\Phi(\mathbf{r})$. It has been claimed that the use of a scalar potential is inappropriate and that the vector potential $\mathbf{A}\cdot\mathbf{p}$ interaction should be used instead.[38] However, it is easy to show that the scalar and vector potential representations lead to nearly identical results at the frequencies of interest, as one would expect from the principle of gauge invariance.[39,40]

A more serious objection is that this approximation ignores the mechanical boundary conditions at the interfaces. Indeed, a straightforward application of the dielectric continuum model leads to a discontinuity in the ionic displacement field at the interfaces, which is not consistent with the microscopic phonon models. However, calculations of scattering rates in quantum wells show that this discrepancy does not lead to significant errors, so that the dielectric continuum model is well suited for transport calculations.[31]

In calculating the electron-phonon Hamiltonian, we will assume that the widths of the collector and emitter barriers are the same. However, experimental structures—including the one we are modeling here—frequently have barriers of unequal width. It is possible to calculate the electron-phonon Hamiltonians for asymmetric double-barrier structures (the formulas are considerably more cumbersome than for symmetric structures) but the dispersion relations and the phonon potentials for the 33-80-45-Å structure are not significantly different from those presented here.[41] For the purposes of calculating the phonon properties we use the emitter barrier thickness on both sides of the well. Since the initial and final wave functions do not possess significant overlap in the collector barrier (see Fig. 1), this is a good approximation for the purposes of calculating the PAT current.

We start with the Lagrangian density of the phonon field:[42–44]

$$\mathcal{L}_{\text{ph}}=\tfrac{1}{2}\dot{\mathbf{w}}^2-\tfrac{1}{2}\omega_T^2\mathbf{w}^2+\tfrac{1}{2}\varepsilon_0\kappa_\infty\nabla\Phi\cdot\nabla\Phi-\gamma\mathbf{w}\cdot\nabla\Phi\ . \tag{3.1}$$

Here $\mathbf{w}(\mathbf{r})=\rho^{1/2}\mathbf{u}(\mathbf{r})$, where $\mathbf{u}(\mathbf{r})$ is the displacement from equilibrium of the positive ions less that of the negative ions, ρ is the reduced mass per unit volume, ε_0 is the permittivity of free space, and γ is defined by

$$\gamma^2=\varepsilon_0(\kappa_0-\kappa_\infty)\omega_T^2=\varepsilon_0\kappa_\infty(\omega_L^2-\omega_T^2)\ , \tag{3.2}$$

where κ_∞ and κ_0 are the high- and low-frequency dielectric constants, respectively, and ω_L and ω_T are the longitudinal and transverse optical phonon frequencies, respectively. It is important to note that the quantities κ_∞, κ_0, ω_L, ω_T, and γ are independent on the material type (e.g., GaAs or AlAs), and are thus functions of z.

The Euler-Lagrange equation for the potential Φ gives the Poisson equation with a z-dependent dielectric function $\varepsilon(\omega;z)$:

$$\nabla\cdot\{\varepsilon(\omega;z)\nabla\Phi\}=0 \tag{3.3}$$

where $\varepsilon(\omega;z)$ is given by the standard form

$$\varepsilon(\omega;z)=\varepsilon_0\kappa_\infty\frac{\omega^2-\omega_L^2}{\omega^2-\omega_T^2}\ . \tag{3.4}$$

Since we have translational invariance in the x-y direction, the potential due to the phonons can be expanded in the form

$$\Phi(\mathbf{r})=\sum_{\mathbf{q}_\parallel}\phi(\mathbf{q}_\parallel)\frac{f(q_\parallel;z)e^{i\mathbf{q}_\parallel\cdot\mathbf{r}_\parallel}}{\sqrt{A}}\ , \tag{3.5}$$

where $\mathbf{q}_\parallel$ is the momentum of the phonon in the x-y plane, $\phi(\mathbf{q}_\parallel)$ is an expansion coefficient, and $f(q_\parallel;z)$ describes the phonon potential in the z direction and satisfies the equation

$$\frac{d}{dz}\left[\varepsilon(\omega;z)\frac{d}{dz}f(q_\parallel;z)\right]-q_\parallel^2 f(q_\parallel;z)\varepsilon(\omega;z)=0\ . \tag{3.6}$$

Equation (3.6) may also be written in an integral form:

$$\int\varepsilon(z;\omega)\left[q_\parallel^2 f^2+\left[\frac{df}{dz}\right]^2\right]dz=0\ , \tag{3.7}$$

where the integral extends over the entire z axis.

The dispersion relations and phonon potentials are found by solving Eq. (3.6).[16] For a double-barrier struc-

ture there are four heterointerfaces and a total of 14 localized phonon modes. These are the LO-like and TO-like confined modes in the well, the LO-like and TO-like confined modes in the two barriers, and eight interface modes. Four of the interface modes are symmetric with respect to the center of the well, while the other four are antisymmetric.

For the LO-like confined modes, $f(q_\parallel;z)$ is given by

$$f(q_\parallel;z)=\sin(\alpha_n z)\ , \tag{3.8}$$

where z is measured from the left side of the confining region and $\alpha_n=n\pi/d$, where d is the width of the confining region with $n=1,2,3,\ldots$. The dispersionless frequency is given by $\varepsilon(\omega;z)=0$, as for the bulk case, where $\varepsilon(\omega;z)$ is the dielectric function for the confining region. Thus the LO-like confined modes in the well have the energy of bulk LO phonons in GaAs, $\hbar\omega\approx 36.2$ meV, while the LO-like confined modes in the barriers have the energy of bulk LO phonons in AlAs, $\hbar\omega\approx 50.1$ meV. The TO-like confined modes do not couple strongly with electrons, and are not considered here.

The dispersion relation for the symmetric interface phonons is given by[16,45]

$$\varepsilon_2^2\tanh(q_\parallel d_2)+\varepsilon_1\varepsilon_2[\tanh(\tfrac{1}{2}q_\parallel d_1)+1] +\varepsilon_1^2\tanh(q_\parallel d_2)\tanh(\tfrac{1}{2}q_\parallel d_1)=0\ , \tag{3.9}$$

where ε_1 is the dielectric constant of the well and spacer layers (GaAs), and ε_2 is the dielectric constant of the barriers (AlAs). To obtain dispersion relations for the antisymmetric interface phonons, simply replace $\tanh(q_\parallel d_1/2)$ by $\coth(q_\parallel d_1/2)$ in Eq. (3.9). In the long-wavelength limit ($q_\parallel\to 0$) the energies of the interface phonons converge to bulk LO- and TO-phonon energies. We can therefore classify interface phonons as TO-like or LO-like depending on their long-wavelength value of energy. It is important to realize, however, that *both* the LO-like and TO-like interface phonons can interact with electrons, though typically the LO-like phonons have a stronger effect.

The function $f(q_\parallel;z)$—which describes the electrostatic potential created by the phonon—has been written out for the case of double-barrier symmetric and antisymmetric interface modes in Ref. 45. In Fig. 2 we plot $f(q_\parallel;z)$ for the four LO-like interface phonons for a structure with an 80-Å well and 33-Å AlAs barriers. A distinction between the two symmetric interface phonons is immediately evident. The potential profile of the phonon in Fig. 2(a) peaks at the outer interface, and we call this the outer symmetric interface phonon. In the long-wavelength limit it has the energy of the bulk GaAs LO phonons: 36.2 meV. The potential profile of the phonon in Fig. 2(b) peaks at the inner interface, and we call this the inner symmetric interface phonon. In the long-wavelength limit it has the energy of the bulk AlAs LO phonons: 50.1 meV. Similarly, the mode depicted in Fig. 2(c) is called the inner antisymmetric interface phonon and has an energy of 36.2 meV in the long-wavelength limit, while the phonon mode depicted in Fig. 2(d) is called the outer antisymmetric interface phonon and has an energy 50.1 meV in the long-wavelength limit.

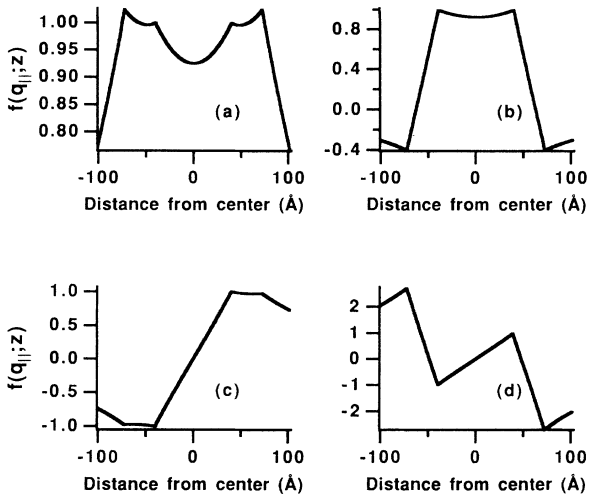

FIG. 2. The function $f(q_\parallel;z)$ for the LO-like interface phonons: (a) the outer symmetric interface phonon, (b) the inner symmetric interface phonon, (c) the inner antisymmetric interface phonon, and (d) the outer antisymmetric interface phonon.

The electron-phonon Hamiltonian is given by $H_{e\text{-ph}}=e\Phi$, where e is the charge of the electron and Φ is the phonon potential. A form of this Hamiltonian valid for all localized modes is derived in the Appendix and is given by

$$H_{e\text{-ph}}=\sum_{\mathbf{q}_\parallel}\frac{\beta(q_\parallel)}{\sqrt{A}}e^{i\mathbf{q}_\parallel\cdot\mathbf{r}_\parallel}f(q_\parallel;z)[a(\mathbf{q}_\parallel)+a^\dagger(-\mathbf{q}_\parallel)]\ , \tag{3.10}$$

where $a^\dagger(-\mathbf{q}_\parallel)$ and $a(\mathbf{q}_\parallel)$ are the creation and annihilation operators for the phonons, and the coupling coefficient $\beta(q_\parallel)$ is given by

$$\beta(q_\parallel)=(e^2\hbar)^{1/2}\left\{\int\frac{\partial\varepsilon(\omega;z)}{\partial\omega}\left[q_\parallel^2 f^2+\left[\frac{df}{dz}\right]^2\right]dz\right\}^{-1/2}\ . \tag{3.11}$$

It is interesting to note that Eqs. (3.10) and (3.11) for the electron-localized phonon Hamiltonian apply not only to double-barrier structures but also to arbitrary heterostructures. Note the similarity between the definition of $\beta(q_\parallel)$ and the phonon dispersion relation as expressed in Eq. (3.7). Because the phonon potential term $f(q_\parallel;z)$ occurs in both the Hamiltonian, Eq. (3.10) and the definition of $\beta(q_\parallel)$, Eq. (3.11), the overall normalization of $f(q_\parallel;z)$ is not important. We can multiply $f(q_\parallel;z)$ by any function of $q_\parallel$ and while the *form* of the Hamiltonian may appear completely different, any physical quantities that are calculated will be unaffected.

For the confined phonons, $\beta(q_\parallel)$ can be reduced to

$$\beta(q_\parallel)=\left[\frac{2e^2\hbar}{\frac{\partial\varepsilon(\omega)}{\partial\omega}d[q_\parallel^2+\alpha_n^2]}\right]^{1/2}\ , \tag{3.12}$$

where d is the length of the confining region. For explicit formulas for the electron-interface phonon Hamiltonians in a double-barrier structure, see Ref. 45.

Figure 3 plots the value of $\beta(q_\parallel)$ for all localized phonon modes for a double-barrier structure with an 80-Å GaAs well and two 33-Å AlAs barriers on a logarithmic scale. In order to obtain a proper sense for which modes are more important, we have calculated $\beta(q_\parallel)$ using a normalized version of $f(q_\parallel;z)$ which satisfies $\int f^2 dz = 1$ and gives $\beta(q_\parallel)$ in dimensions of (energy) (length)$^{3/2}$. The interface phonon modes are labeled according to the notation of Kim *et al.*,[45] which is summarized in Table I. In Fig. 3(a) we show $\beta(q_\parallel)$ for the antisymmetric interface modes. Note that the two LO-like modes ω_{a2+} and ω_{a1-} have the largest values of $\beta(q_\parallel)$ at low $q_\parallel$. In both cases $\beta(q_\parallel) \propto (1/q_\parallel)^{1/2}$ at small values of $q_\parallel$. The two TO-like modes ω_{a2-} and ω_{a1+} are not nearly as important at low $q_\parallel$.

In Fig. 3(b) we show $\beta(q_\parallel)$ for the symmetric interface modes and the confined modes of the system. The LO-like outer symmetric mode ω_{s1+} is largest over most of the range of $q_\parallel$. It diverges as $1/q_\parallel$ at low values of $q_\parallel$. The TO-like outer symmetric mode ω_{s2+} is also quite strong, and diverges as $(1/q_\parallel)^{1/2}$ at small values of $q_\parallel$. The two inner symmetric modes are weaker, with the TO-like mode going to zero proportional to $q_\parallel$ at small values of $q_\parallel$. The two confined modes are almost constant as a function of $q_\parallel$ since, for the range covered here, $\alpha_n > q_\parallel$. The confined mode in the well (ω_{cw}) is stronger than the confined mode in the barrier (ω_{cb}) because the α_n for the confined mode in the well is larger than the α_n for the confined mode in the barrier.

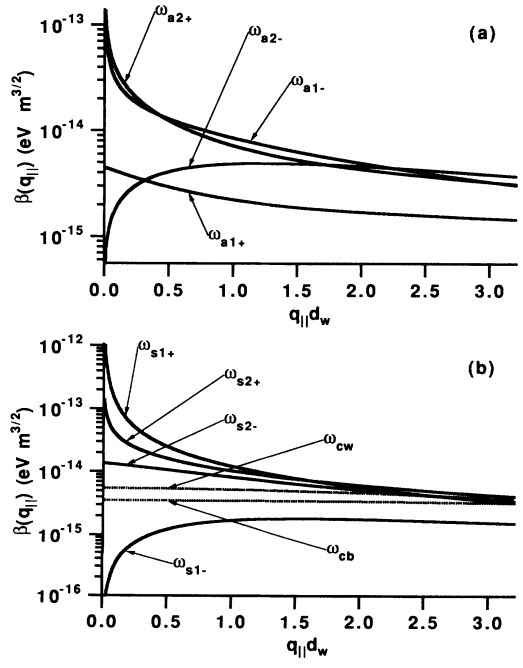

FIG. 3. The coupling coefficient β vs $q_\parallel d_1$, (a) for the antisymmetric interface phonons, and (b) for the symmetric interface phonons and confined phonons.

It is important to realize that we cannot immediately decide from this graph which localized modes will contribute the most to the PAT current. In Sec. IV we shall find that the current due to PAT is roughly proportional to $\beta^2(q_\parallel)|\lambda(q_\parallel)|^2$, where $\lambda(q_\parallel)$ is an overlap integral between the phonon potential and the electronic states. The overlap integral is largest for the LO-like inner symmetric mode and the confined modes in the well, which raises their contribution to the current, while for the LO-like outer symmetric interface mode the overlap integral is very small, dramatically reducing the current due to this mode.

The properties of the interface modes are summarized in Table I. In the first and second columns we have designated the phonons using the notation of Kim *et al.*[45] and Mori, Taniguchi, and Hamiguchi.[17] In the third column we have given the energy of the phonon in the long-wavelength limit. We then can define the phonon mode as LO-like or TO-like. In the fifth column we show the dependence of the coupling coefficient $\beta(q_\parallel)$ on the phonon wave vector $q_\parallel$ in the long-wavelength limit, i.e., as $q_\parallel \rightarrow 0$. Since most of the phonons emitted by the tunneling electrons have $q_\parallel d_1 < 1$ and $q_\parallel d_2 < 1$, this limit strongly determines which type of phonon will contribute most to the PAT current.

In addition to the localized phonon modes just discussed, we should also consider the bulk LO phonon in the GaAs contact regions. Because these modes cannot penetrate the AlAs layer, they are typically called half-space modes as they exist on only one side of the interface.[24] For PAT, the half-space modes in the collector region are of no importance. The initial and final electronic wave functions barely penetrate into the collector, and the overlap integral between the electronic wave functions and the phonon potential will be negligible.

On the other hand, the half-space LO modes in the emitter can be very important in many structures, and they should be included in any calculation of PAT. One method of doing this is to treat the half-space modes as confined modes in the emitter, with $\alpha_n = n\pi/L_e$, where L_e is the length of the emitter. One can then let $L_e \rightarrow \infty$ and convert the sum over n to an integral. However, since most of the overlap with the electronic wave functions occurs within 200 Å of the emitter barrier, in our structure we can simply let $L_e = 500$ Å, sum over n from one to 20 and obtain a very close approximation ($< 1\%$ error) to the $L_e \rightarrow \infty$ calculation.

IV. CALCULATION OF PHONON-ASSISTED TUNNELING CURRENTS

Inserting the electron-phonon Hamiltonian Eq. (3.10) and the electronic states Eq. (2.2) into the Fermi golden rule Eq. (2.1) yields the emission rate:

$$W(i \rightarrow f) = \frac{2\pi}{A\hbar} \beta^2(q_\parallel) |\lambda(q_\parallel)|^2 \delta_{\mathbf{k}_\parallel - \mathbf{k}'_\parallel - \mathbf{q}_\parallel} \delta(E_i - E_f - \hbar\omega) , \tag{4.1}$$

TABLE I. Summary of interface mode properties.

Kim *et al.*	Mori, Taniguchi, and Hamiguchi	$\hbar\omega(q_\parallel \to 0)$	Name	$q_\parallel$ dependence of $\beta(q_\parallel)$ as $q_\parallel \to 0$
ω_{s1-}	S_0^-	33.1 meV	TO-like inner symmetric	$q_\parallel$
ω_{s1+}	S_0^+	36.2 meV	LO-like outer symmetric	$1/q_\parallel$
ω_{s2+}	S_1^+	44.8 meV	TO-like outer symmetric	$(1/q_\parallel)^{1/2}$
ω_{s2-}	S_1^-	50.1 meV	LO-like inner symmetric	constant
ω_{a1+}		33.1 meV	TO-like outer antisymmetric	constant
ω_{a1-}		36.2 meV	LO-like inner antisymmetric	$(1/q_\parallel)^{1/2}$
ω_{a2-}		44.8 meV	TO-like inner antisymmetric	$q_\parallel$
ω_{a2+}		50.1 meV	LO-like outer antisymmetric	$(1/q_\parallel)^{1/2}$

where $\hbar\omega$ is the phonon energy, which is a function of $q_\parallel$ for the interface modes and is constant for the confined phonons. $\lambda(q_\parallel)$ is the overlap integral of the phonon potential with the electronic states:[16]

$$\lambda(q_\parallel)=\int \varphi_f^*(z) f(q_\parallel;z)\varphi_i(z)dz \ . \tag{4.2}$$

This rate may then be inserted into the current formula Eq. (2.3) to yield

$$J(V)=\frac{e}{4\pi^3\hbar}\int [1-f_w(\mathbf{k}'_\parallel)]d\mathbf{k}'_\parallel \int_{-\pi}^{\pi} d\phi \int_0^{k_{\parallel F}} k_\parallel dk_\parallel \beta^2(q_\parallel)|\lambda(q_\parallel)|^2\delta(E_i-E_f-\hbar\omega) \ , \tag{4.3}$$

where ϕ is the angle between $\mathbf{k}_\parallel$ and $\mathbf{k}'_\parallel$ as shown in Fig. 4. In previous papers we integrated first over $\mathbf{k}'_\parallel$ in order to obtain an expression for the scattering rate $W(\mathbf{k}_\parallel)$.[14–16] If we are only interested in calculating the current, however, it is more efficient to integrate over $\mathbf{k}_\parallel$ first. Using conservation of energy and momentum

$$E_i-E_f-\hbar\omega=\frac{\hbar^2}{2m^*}(k_\parallel^2-k_\parallel'^2)-(\hbar\omega-\Delta E_z)=0 \tag{4.4}$$

and

$$q_\parallel^2=k_\parallel^2+k_\parallel'^2-2k_\parallel k'_\parallel\cos(\phi) \ , \tag{4.5}$$

where ΔE_z is the z-energy difference between the emitter state and the well state, we can integrate over the initial electronic states to yield a central result of this paper:

$$J(V)=\frac{em^*}{\pi^2\hbar^3}\int_0^{\pi} d\phi \int_{k'_{\parallel\min}}^{k'_{\parallel\max}} k'_\parallel dk'_\parallel \beta^2(Q_\parallel)|\lambda(Q_\parallel)|^2 \ . \tag{4.6}$$

The limits of the integration are given by

$$k'^2_{\parallel\max}=\begin{cases} k_F^2+\xi & \text{if } k_F'^2\le k_F^2+\xi \\ k_F'^2 & \text{if } k_F'^2\ge k_F^2+\xi \end{cases} \tag{4.7}$$

and

$$k'^2_{\parallel\min}=\begin{cases} \xi & \text{if } k_F'^2\le \xi \\ k_F'^2 & \text{if } k_F'^2\ge \xi \ , \end{cases} \tag{4.8}$$

where k_F is the Fermi wave vector of the initial (emitter) state, k'_F is the Fermi wave vector of the final (well) state, and

$$\xi=\frac{2m^*}{\hbar^2}(\Delta E_z-\hbar\omega) \ . \tag{4.9}$$

The quantities $Q_\parallel$ and $K_\parallel$ are the wave vectors of the emitted phonon and the initial electron for a given final electron wave vector $k'_\parallel$ and angle ϕ, and are specified by

$$Q_\parallel^2=k_\parallel'^2+K_\parallel^2-2k'_\parallel K_\parallel\cos(\phi) \tag{4.10}$$

and

$$K_\parallel^2=k_\parallel'^2+\frac{2m^*}{\hbar^2}[\hbar\omega(Q_\parallel)-\Delta E_z] \ . \tag{4.11}$$

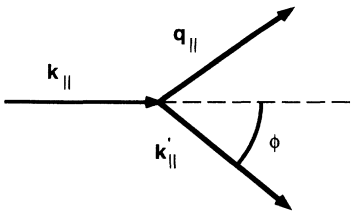

FIG. 4. Dynamics of the phonon emission process projected into the x-y plane; ϕ is the angle between the incoming electron and the scattered electron projected onto the plane of the interfaces.

Equation (4.6) for $J(V)$ is a general formula for the current due to PAT, valid for all confined and interface phonon modes. It represents a considerable simplification over previous expressions in that only (a maximum of) three numerical integrations need to be performed. It also clearly expresses the fact that the PAT current is proportional to the coupling coefficient $\beta(Q_\parallel)$ and the overlap integral $\lambda(Q_\parallel)$.

The voltage dependence of $J(V)$ enters into the formula most strongly through the dependence of the ΔE_z in Eqs. (4.9) and (4.11) on the voltage. On the other hand, the overlap integral $\lambda(Q_\parallel)$ has a relatively weak dependence on the voltage. For the interface modes, $K_\parallel$ and $Q_\parallel$ are related in a nontrivial manner through $\hbar\omega(Q_\parallel)$, and thus Eqs. (4.10) and (4.11) must be solved simultaneously for a given final electron wave vector $k'_\parallel$ and angle ϕ. For the confined phonons $\hbar\omega$ is dispersionless (not a function of $q_\parallel$), so, using the functional form of $\beta(q_\parallel)$ [Eq. (3.12)], we can integrate Eq. (4.6) to find an analytical expression for the current due to the confined modes:

$$J(V)=\sum_n \frac{e\gamma_c^2\lambda_n^2 m^*}{4\pi d\hbar^3\alpha_n^2}\left\{\left[4k'^2_{\parallel\max}\alpha_n^2+\left[\alpha_n^2+\frac{2m^*}{\hbar^2}(\hbar\omega-\Delta E_z)\right]^2\right]^{1/2}-\left[4k'^2_{\parallel\min}\alpha_n^2+\left[\alpha_n^2+\frac{2m^*}{\hbar^2}(\hbar\omega-\Delta E_z)\right]^2\right]^{1/2}\right\}, \tag{4.12}$$

where λ_n is the overlap integral, which now depends solely on n, and the γ_c is defined by

$$\gamma_c=\left[\frac{2\hbar e^2}{\frac{\partial\varepsilon(\omega)}{\partial\omega}}\right]^{1/2}=\left[\frac{\hbar\omega e^2}{\varepsilon_0}\left[\frac{1}{\kappa_\infty}-\frac{1}{\kappa_0}\right]\right]^{1/2}. \tag{4.13}$$

Typically, the contribution from the lowest-order confined mode with $n=1$ is stronger than the higher-order modes.[46] A simple and reasonably accurate ($<10\%$ error) approximation to Eq. (4.12) can be made by assuming $\alpha_n^2 \gg |(2m^*/\hbar^2)(\hbar\omega-\Delta E_z)|$ and $\alpha_n^2 \gg k'^2_{\parallel\max,\min}$, which is equivalent to setting $\alpha_n^2+q_\parallel^2 \Rightarrow \alpha_n^2$ in Eq. (3.12).[16] This yields the remarkably simple result

$$J(V)\approx\frac{e\gamma_c^2 m^*}{2\pi d\hbar^3}[k'^2_{\parallel\max}-k'^2_{\parallel\min}]\sum_n\frac{\lambda_n^2}{\alpha_n^2}. \tag{4.14}$$

This simple analytical expression can be used to compare the strength of different confined modes. It is a very good approximation for voltages near the peak of the PAT current (where $\hbar\omega\approx\Delta E_z$), but breaks down at high voltages where $\hbar\omega \ll \Delta E_z$.[47]

V. DISCUSSION

Figure 5 shows a graph of the PAT current due to each optical-phonon mode. For simplicity we have set $f_w(\mathbf{k}'_\parallel)=0$ in these calculations, so that the effects of Pauli exclusion and charge buildup in the well are not included. The effects of these processes on calculated current-voltage curves are shown in Ref. 9.

Figure 5(a) shows the currents plotted on a logarithmic scale, so that the smaller contributions can be seen. The current due to the confined modes in the collector barrier (labeled $\omega_{\rm cbc}$) is very small due to the very small overlap of the wave functions in the collector barrier. The current due to the confined modes in the emitter barrier (labeled $\omega_{\rm cbe}$) is larger, but the overlap of the wave functions in the barriers is still too small for the confined modes in the barrier to have much effect on the current. This observation appears to be true for almost any double-barrier structure that can be designed, and previous authors who claimed to have observed tunneling assisted by phonons in the barriers were actually looking at interface phonons.[1,2]

It is not surprising that currents due to TO-like inner symmetric phonons (ω_{s1-}), and TO-like outer antisymmetric phonons (ω_{a1+}) are small. As shown in Fig. 3, both types have small $\beta(q_\parallel)$ over the entire range of $q_\parallel$ values. It is more surprising that both the LO-like and TO-like outer symmetric phonons (ω_{s1+}) and (ω_{s2+}) do not contribute much to the current. Here the overlap in-

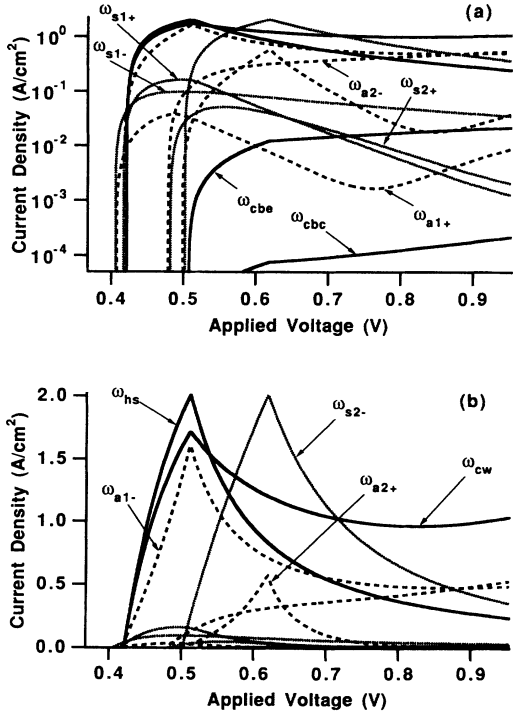

FIG. 5. Contributions to the phonon-assisted tunneling current from each of the phonon modes: (a) The current on a logarithmic scale with the smaller contributions labeled. (b) The current on a linear scale with the larger contributions labeled.

tegral is critical. As $q_{\|}$ goes to zero, the potential function of the outer symmetric phonons $f(q_{\|};z)$ goes to a constant, independent of z (see Fig. 2). The overlap integral $\lambda(q_{\|})$ is then approximately proportional to $\int dz\, \varphi_f^*(z)\varphi_i(z)$. Since the initial and final electronic states are eigenfunctions of the same Hamiltonian, however, they are orthogonal, and the overlap integral must vanish as $q_{\|}\rightarrow 0$. For finite values of $q_{\|}$ the overlap integral is still quite small, and the contributions to the overall current from these two modes are negligible. In order to model this effect correctly, it is imperative to do two things: first, we must construct properly orthogonal electronic states, and, second, the overlap integral must be extended over both the well and the emitter of the device. If these two steps are not taken, the current due to the outer symmetric modes may be greatly overestimated.[17]

Note that the TO-like inner symmetric mode (ω_{a2-}) makes the largest contribution of any of the TO-like modes. As seen in Fig. 3, this mode has a very low coupling coefficient at small $q_{\|}$, but for large $q_{\|}$ its coupling coefficient is the largest of any of the antisymmetric modes. This behavior is reflected in the *I-V* curve. At low voltages, where $\Delta E_z \approx \hbar\omega$ and $q_{\|}$ is small, the ω_{a2-} mode does not make a large contribution to the current. At higher voltages, however, where $\Delta E_z > \hbar\omega$ and $q_{\|}$ is larger, the ω_{a2-} mode contributes much more strongly to the current.

The other five types of phonon modes—the two LO-like antisymmetric modes, the LO-like inner symmetric modes, the confined modes in the well, and the half-space modes in the emitter—all make sizable contributions to the PAT current, as seen in Fig. 5(b). The LO-like inner symmetric mode makes one of the largest contributions, mainly because the overlap between its potential profile and the electronic states is particularly favorable in this structure. Figure 5 plots the contributions from each phonon mode separately in order to see which modes dominate the PAT current. To find the total PAT current through the double-barrier structure, the contributions from each phonon mode are simply added together. To compare with experiment, however, both the broadening of the electronic states and the buildup of charge in the well must be taken into account as described in Ref. 9.

In Ref. 9, the overlap integral between the phonon potential and the electronic wave functions was calculated for the well and barrier alone, i.e., the contribution to the overlap integral from the emitter region was not included. This does not significantly affect the calculated current due to the confined modes in the well and the inner symmetric interface phonons. On the other hand, neglecting the emitter region in the overlap calculation leads to a substantial overestimation of the PAT current due to LO-like and TO-like outer symmetric modes, while the current from the antisymmetric phonons is underestimated. To understand why a strong contribution from the LO-like and TO-like outer symmetric phonons was not observed in experiment, it was previously speculated that screening of phonons by electrons in the emitter might reduce the strength of these modes. After including the overlap integral in the emitter, however, the strength of the outer symmetric phonons is greatly reduced, and we no longer need to appeal to screening to suppress the contributions from these two modes. Of course, if a structure is designed so that the electron density in the well or emitter is large, or the electron gas in the emitter is effectively three dimensional, we would expect screening to be important.

In conclusion, we find good agreement between theory and experiment in both forward and reverse biases by adding up the contributions of *all* the phonon modes, with the effects of charge buildup in the well and broadening of the electronic states included.[48] We have also looked at other GaAs/AlAs double-barrier structures—with different well and barrier thicknesses—and found good agreement between the measured PAT currents and theoretical calculations.[48]

ACKNOWLEDGMENTS

We thank R. Lake and C. R. Wallis for helpful conversations and also acknowledge the support of the National Science Foundation through Grant No. DMR-9208381. One of us (P.J.T.) acknowledges the support of the Katherine Stern Foundation.

APPENDIX: THE DERIVATION OF THE ELECTRON-PHONON HAMILTONIAN

In this appendix we derive Eqs. (3.10) and (3.11) for the electron-phonon Hamiltonian. Using the Lagrangian density Eq. (3.1) we form the canonical momentum density $\pi(\mathbf{r})$ we write the Hamiltonian density:

$$\mathcal{H}_{\rm ph}=\tfrac{1}{2}\pi^2+\tfrac{1}{2}\omega_T^2\mathbf{w}^2-\tfrac{1}{2}\varepsilon_0\kappa_\infty\nabla\Phi\cdot\nabla\Phi+\gamma\mathbf{w}\cdot\nabla\Phi\ . \tag{A1}$$

The phonon potential and the lattice displacement field are not independent variables, but are related through the Euler-Lagrange equations for $\mathbf{w}$:

$$\frac{\partial^2\mathbf{w}}{\partial t^2}=-\omega_T\mathbf{w}-\gamma\nabla\Phi\ , \tag{A2}$$

or, assuming harmonic time dependence,

$$\mathbf{w}=\frac{\gamma\nabla\Phi}{\omega^2(q_{\|})-\omega_T^2}\ , \tag{A3}$$

so that the Hamiltonian density may be written as

$$\mathcal{H}_{\rm ph}=\tfrac{1}{2}\pi^2+\tfrac{1}{2}\omega^2(q_{\|})\mathbf{w}^2+\frac{1}{2}\frac{[\omega^2(q_{\|})-\omega_T^2]^2}{\gamma^2}\varepsilon(z;\omega)\mathbf{w}^2\ . \tag{A4}$$

Here $\omega(q_{\|})$ is the frequency of the phonons and is given by the solution to the appropriate dispersion relation.

Expanding in normal coordinates, both the displacement field and the canonical momentum density can be written in a manner similar to the electrostatic potential:

$$\mathbf{w}(\mathbf{r})=\sum_{\mathbf{q}_{\|}} w(\mathbf{q}_{\|})g(q_{\|};z)\hat{\mathbf{e}}(\mathbf{q}_{\|};z)\frac{e^{i\mathbf{q}_{\|}\cdot\mathbf{r}_{\|}}}{\sqrt{A}} \tag{A5}$$

and

$$\pi(\mathbf{r})=\sum_{\mathbf{q}_\parallel}\pi(\mathbf{q}_\parallel)g(q_\parallel;z)\hat{\mathbf{e}}(\mathbf{q}_\parallel;z)\frac{e^{i\mathbf{q}_\parallel\cdot\mathbf{r}_\parallel}}{\sqrt{A}}\ , \tag{A6}$$

where $\pi(\mathbf{q}_\parallel)=\partial w(\mathbf{q}_\parallel)/\partial t$, $\hat{\mathbf{e}}(\mathbf{q}_\parallel;z)$ is the polarization vector, and $g(q_\parallel;z)$ is a normalized function (i.e., $\int|g(q_\parallel;z)|^2dz=1$) which characterizes the z dependence of the ionic displacements. Integrating over all space yields the "bare" phonon Hamiltonian:

$$H_{\rm ph}=\sum_{\mathbf{q}_\parallel}\left[\tfrac{1}{2}\pi(\mathbf{q}_\parallel)\pi(-\mathbf{q}_\parallel)+\tfrac{1}{2}\omega^2(q_\parallel)w(\mathbf{q}_\parallel)w(-\mathbf{q}_\parallel)+\tfrac{1}{2}w(\mathbf{q}_\parallel)w(-\mathbf{q}_\parallel)\times\int\frac{[\omega^2(q_\parallel)-\omega_T^2]^2}{\gamma^2}\varepsilon(\omega;z)g^2(q_\parallel;z)dz\right]\ . \tag{A7}$$

For the confined modes, since $\varepsilon(\omega)=0$ over the region of interest the last term is easily seen to vanish. For the interface modes, more work is required. Using the expansion of the phonon potential [Eq. (3.5)] and the expansion of the displacement field [Eq. (A5)], we derive the following relation:

$$wg=\frac{\gamma\phi}{\omega^2-\omega_T^2}\left[q_\parallel^2f^2+\left[\frac{df}{dz}\right]^2\right]^{1/2}\ . \tag{A8}$$

Squaring both sides and integrating over all space yields

$$w^2=\phi^2\int\frac{\gamma^2}{(\omega^2-\omega_T^2)^2}\left[q_\parallel^2f^2+\left[\frac{df}{dz}\right]^2\right]dz\ . \tag{A9}$$

It is important to remember that γ and ω_T are both functions of z, and cannot be taken outside the integral. We can combine Eqs. (A8) and (A9) to find

$$g^2=\frac{\eta\gamma^2}{(\omega^2-\omega_T^2)^2}\left[q_\parallel^2f^2+\left[\frac{df}{dz}\right]^2\right]\ , \tag{A10}$$

where η is a constant [basically the integral in Eq. (A9)] which depends only on the normalization of $f(q_\parallel;z)$. Using Eq. (A10) we can now rewrite the last term of the phonon Hamiltonian of Eq. (A7) in the form:

$$\frac{\eta w(\mathbf{q}_\parallel)w(-\mathbf{q}_\parallel)}{2}\int\varepsilon(z;\omega)\left[q_\parallel^2f^2+\left[\frac{df}{dz}\right]^2\right]dz\ . \tag{A11}$$

This expression is equivalent to the alternate form of the dispersion relation Eq. (3.7), and it is therefore equal to zero.

Since the last term in Eq. (A7) drops out for both confined and interface modes, the Hamiltonian can generally be expressed in the form

$$H_{\rm ph}=\sum_{\mathbf{q}_\parallel}\tfrac{1}{2}\pi(\mathbf{q}_\parallel)\pi(-\mathbf{q}_\parallel)+\tfrac{1}{2}\omega^2(q_\parallel)w(\mathbf{q}_\parallel)w(-\mathbf{q}_\parallel)\ . \tag{A12}$$

We can express $H_{\rm ph}$ quantum mechanically by writing $\pi(\mathbf{q}_\parallel)$ and $w(\mathbf{q}_\parallel)$ in terms of phonon creation and annihilation operators:

$$\pi(\mathbf{q}_\parallel)=\frac{1}{i}\left[\frac{\hbar\omega(q_\parallel)}{2}\right]^{1/2}[a(\mathbf{q}_\parallel)-a^\dagger(\mathbf{q}_\parallel)] \tag{A13}$$

and

$$w(\mathbf{q}_\parallel)=\left[\frac{\hbar}{2\omega(q_\parallel)}\right]^{1/2}[a(\mathbf{q}_\parallel)+a^\dagger(\mathbf{q}_\parallel)]\ , \tag{A14}$$

so that $H_{\rm ph}$ is expressed in the standard form

$$H_{\rm ph}=\sum_{\mathbf{q}_\parallel}\hbar\omega(q_\parallel)[a^\dagger(\mathbf{q}_\parallel)a(\mathbf{q}_\parallel)+\tfrac{1}{2}]\ . \tag{A15}$$

Now that we have the bare phonon Hamiltonian, we can go back and derive the electron-phonon interaction. The interaction Hamiltonian can be written $H_{e\text{-ph}}=e\Phi(r)$, where $\Phi(r)$ is the electrostatic potential associated with the phonons. Expanding the phonon potential as in Eq. (3.5), and using the relation between $\phi(\mathbf{q}_\parallel)$ and $w(\mathbf{q}_\parallel)$ presented in Eq. (A9), we have

$$H_{e\text{-ph}}=e\sum_{\mathbf{q}_\parallel}\frac{w(\mathbf{q}_\parallel)}{\left\{\int\left[\frac{\gamma}{\omega^2-\omega_T^2}\right]^2\left[q_\parallel^2f^2+\left[\frac{df}{dz}\right]^2\right]dz\right\}^{1/2}}\times\frac{e^{\mathbf{q}_\parallel\cdot\mathbf{r}_\parallel}}{\sqrt{A}}\ . \tag{A16}$$

Using the standard form for the dielectric function [i.e., Eq. (3.4)], and expression $w(\mathbf{q}_\parallel)$ in terms of the creation and annihilation operators as in Eq. (A14), we arrive at the general expression for the electron-phonon Hamiltonian valid for all localized phonons and given in Eqs. (3.10) and (3.11).

[1] V. J. Goldman, D. C. Tsui, and J. E. Cunningham, Phys. Rev. B **36**, 7635 (1987).

[2] M. L. Leadbeater, E. S. Alves, L. Eaves, M. Henini, O. H. Hughes, A. Celeste, J. C. Portal, G. Hill, and M. A. Pate, Phys. Rev. B **39**, 3438 (1989).

[3] A. Celeste, L. A. Cury, J. C. Portal, M. Allovon, D. K. Maude, L. Eaves, M. Davies, M. Heath, and M. Maldonado, Solid State Electron. **32**, 1191 (1989).

[4] S. Ben Amor, K. P. Martin, J. J. L. Rascol, R. J. Higgins, R. C. Potter, A. A. Lakhani, and H. Hier, Appl. Phys. Lett. **54**, 1908 (1989).

[5] G. S. Boebinger, A. F. J. Levi, S. Schmitt-Rink, A. Passner, L. N. Pfeiffer, and K. W. West, Phys. Rev. Lett. **65**, 235 (1990).

[6] H.-Z. Zheng, F.-H. Yang, and Z.-G. Chen, Phys. Rev. B **42**, 5270 (1990).

[7] J. G. Chen, C. H. Yang, M. J. Yang, and R. A. Wilson, Phys. Rev. B **43**, 4531 (1991).

[8] Y. Galvao Gobato, F. Chevoir, J. M. Berroir, P. Bois, Y.

Guldner, J. Nagle, J. P. Vieren, and B. Vinter, Phys. Rev. B **43**, 4843 (1991).
[9]P. J. Turley, C. R. Wallis, S. W. Teitsworth, W. Li, and P. K. Bhattacharya, Phys. Rev. B **47**, 12 640 (1993).
[10]N. S. Wingreen, K. W. Jacobsen, and J. W. Wilkins, Phys. Rev. Lett. **61**, 1396 (1988).
[11]F. Chevoir and B. Vinter, Appl. Phys. Lett. **55**, 1859 (1989).
[12]P. Hyldgaard and A. Jauho, J. Phys. Condens. Matter **2**, 8725 (1990).
[13]J. A. Støvneng, E. H. Haug, P. Lipavsky, and V. Spricka, Phys. Rev. B **44**, 13 595 (1991).
[14]P. J. Turley and S. W. Teitsworth, Phys. Rev. B **44**, 8181 (1991).
[15]P. J. Turley and S. W. Teitsworth, Phys. Rev. B **44**, 12 959 (1991).
[16]P. J. Turley and S. W. Teitsworth, J. Appl. Phys. **72**, 2356 (1992).
[17]N. Mori, K. Taniguchi, and C. Hamiguchi, Semicond. Sci. Technol. **7**, B83 (1992).
[18]N. Zou and K. A. Chao, Phys. Rev. Lett. **69**, 3224 (1992).
[19]P. Roblin and W.-R. Liou, Phys. Rev. B **47**, 2146 (1993).
[20]R. Lake, G. Klimeck, and S. Datta, Phys. Rev. B **47**, 6427 (1993).
[21]F. Chevoir and B. Vinter, Phys. Rev. B **47**, 7260 (1993).
[22]C. H. Grein, E. Runge, and H. Ehrenreich, Phys. Rev. B **47**, 12 590 (1993).
[23]P. Cheng and J. S. Harris, Jr., Appl. Phys. Lett. **55**, 572 (1989).
[24]N. Mori and T. Ando, Phys. Rev. B **40**, 6175 (1989).
[25]J. Chen, J. G. Chen, C. H. Yang, and R. A. Wilson, J. Appl. Phys. **70**, 3131 (1991).
[26]E. T. Koenig, B. Jogai, M. J. Paulus, C. I. Huang, and C. A. Bozada, J. Appl. Phys. **68**, 3425 (1990).
[27]M. C. Payne, J. Phys. C **19**, 1145 (1986).
[28]P. J. Turley and S. W. Teitsworth (unpublished).
[29]K. Huang and B. Zhu, Phys. Rev. B **38**, 13 377 (1988).
[30]J. Menendez, J. Lumin. **44**, 285 (1989).
[31]P. Lugli, E. Molinari, and H. Rücker, Superlatt. Microstruct. **10**, 471 (1991).
[32]H. Rücker, E. Molinari, and P. Lugli, Phys. Rev. B **44**, 3463 (1991).
[33]A. A. Lucas, E. Kartheuser, and R. G. Badro, Phys. Rev. B **2**, 2488 (1970).
[34]J. L. Licari and R. Evrard, Phys. Rev. B **15**, 2254 (1977).
[35]L. Wendler, Phys. Status Solidi B **129**, 513 (1985).
[36]K. W. Kim, M. A. Stroscio, A. Bhatt, R. Mickevicius, and V. V. Mitin, J. Appl. Phys. **70**, 319 (1991).
[37]X. X. Liang, J. Phys. Condens. Matter **4**, 9869 (1992).
[38]B. K. Ridley and M. Babiker, Phys. Rev. B **43**, 9096 (1991).
[39]P. J. Turley (unpublished).
[40]M. Babiker, N. C. Constantinou, and B. K. Ridley, Phys. Rev. B **48**, 2236 (1993).
[41]P. J. Turley and S. W. Teitsworth (unpublished).
[42]K. J. Nash, Phys. Rev. B **46**, 7723 (1992).
[43]M. Born and K. Huang, *Dynamical Theory of Crystal Lattices* (Clarendon, Oxford, 1954).
[44]R. Evrard, in *Polarons in Ionic Crystals and Polar Semiconductors,* edited by J. T. Devreese (Elsevier, New York, 1972).
[45]K. W. Kim, A. R. Bhatt, M. A. Stroscio, P. J. Turley, and S. W. Teitsworth, J. Appl. Phys. **72**, 2282 (1992).
[46]P. J. Turley and S. W. Teitsworth, Phys. Rev. B **44**, 3199 (1991).
[47]S. W. Teitsworth, P. J. Turley, C. R. Wallis, W. Li, and P. K. Bhattacharya, Semicond. Sci. Technol. **9**, 508 (1994).
[48]P. J. Turley, Ph.D. thesis, Duke University, 1994.